❏ 2621

Particle swarm optimization based multilevel MRI compression using compressive sensing

Tariq Tashan, Ahmed K. Kadhim
Department Electrical Engineering, College of Engineering, Mustansiriyah University, Baghdad, Iraq

Article Info

ABSTRACT

A multilevel compression method, for magnetic resonance imaging (MRI) images, is presented in this paper. First, the image is segmented into frames of equal size. Then, the sparsity of each frame is computed. Based on the sparsity index value, each frame is compressive sensing (CS) compressed/reconstructed at one level of four. Particle swarm optimization (PSO) is used to optimize the amount of information to be used in the CS reconstruction process, and to optimize the sparsity thresholds, that separate the different compression levels. Two-dimensional sigmoid function is suggested as a fitness function for the PSO. Six MRI images are used to evaluate the performance of the proposed method. The results show considerable gain in both peak signal to noise ratio (PSNR) and compression level (CL), when compared to single level compression, which is commonly considered in the literature.

Corresponding Author:

Tariq Tashan
Department Electrical Engineering, College of Engineering, Mustansiriyah University
Baghdad, Iraq
Email: tariq.tashan@uomustansiriyah.edu.iq

1. INTRODUCTION

Compressive sensing (CS) is a very efficient tool for signal compression, since it can sample the signal under the Nyquist rate as stated in [1] and [2]. However, this is only possible if the signal is sparse, where the incoherence property is satisfied. The magnetic resonance imaging (MRI) images as other types of images require compression. These images are not necessarily sparse in the time domain, but they are sparser in other domains like the discrete cosine transform (DCT), the discrete Fourier transform, or the wavelet transform (WT) [3], [4]. An MRI image has different nature other than ordinary images, it contains areas of high sparsity and areas of low sparsity, where high details occur. From image compression perspective, it is not wise to compress the whole image as one frame, using the same compression ratio. A multilevel compression is more proper to compress each frame in the image with respect to its sparsity content.

The CS method has many applications in different trends in previous studies. A comparative analysis of different transforms is presented in [4], the analysis shows that the DCT outperforms other transforms for grey images, while the Haar WT is better for coloured images. A hybrid method for MRI CS-based compression is presented in [5], the method employs the Walsh Hadamard transform and the discrete WT, to provide a sparse domain for the CS. A CS and deep learning method are employed for quantitative MRI reconstruction [6]. A CS MRI image reconstruction is presented in [7], the method adopts the empirical WT as a sparse feature domain and the grey wolf optimizer, to tune the method parameters. The CS is used with dual-tree complex WT to reconstruct an image, by comparing the distorted image measurements to a reference image [8]. A CS-based compression is suggested in [9], the algorithm divides the images into blocks, each block location is found optimally, then sampled differently using specific measurement matrix.

A high speed compression is proposed, by reducing the optical signal size using CS [10]. A projection driven block-based CS recovery algorithm is proposed in [11], to provide more sparsity in the wavelet domain, the algorithm is designed to achieve a focused image among other unfocused images. A CS-based compression for video and image is suggested in [12], the sparsity is adaptively measured in this method. A hyper-chaotic algorithm with 2D CS is used for encryption-compression scheme [13]. Rearranged wavelet coefficients are used with CS for image compression in [14]. An image compression algorithm that employs CS for infrared image, is suggested in [15]. First, block-sparsity is used to represent the small target image, then the correlated source vector of the image is modeled using Bayesian framework. Three recovery methods are explored for CS-based MRI image recovery, Basis Pursuit, Matching Pursuit and Orthogonal Matching Pursuit [16]. CS is used in 3D multi-channel data method for MRI image reconstruction in [17], due to the parallel reconstruction, the processing time gain is the main advantage of the method. Many compression methods as mentioned above use fixed compression ratio for the entire image [18]-[20]. A non-uniform sparsity constraint methods are proposed in [21], [22], the methods suggest splitting the MRI image in the frequency domain to 5 regions, based on the sparsity level of each region. In [23], another algorithm that uses adaptive sparsity CS per block is proposed. Two approaches are considered to set the samples number per block, where the data presented in the DCT domain. Tahsan and Azawi [24] propose a multi-level MRI image compression using CS, six different MRI images are considered, each image is segmented into blocks, then the DCT is computed, based on the sparsity in the block, the compression CS level is chosen. The results show significant better compression, when compared to linear compression for the whole image.

The work here presents a continuation of the proposed algorithm in [24], where the thresholds that define the different four compression levels are selected experimentally, and the amount of information for CS in each level also experimentally selected. The contribution in this paper is by automatically computing these thresholds using the particle swarm optimization (PSO) algorithm, which searches for the optimal value of these thresholds, based on the best fitness function. The fitness function can be either a target compression level, where the PSO tends to find the thresholds of the highest PSNR, or the fitness function can be a target PSNR, where the PSO tends to find the thresholds of the highest compression level.

The rest of the paper is organized as follows: section 2 addresses the CS theoretical background, section 3 explains the PSO theory, section 4 presents the proposed method, section 5 describes the fitness function, section 6 adresses the results and discussion, while section 7 presents the main conclusions.

2.   CS THEORY

The CS simply means sampling the signal under the Nyquist rate and can be described mathematically as follows: Assuming that X is a discrete signal, which can be expressed in different sparse domain S using transformation matrix Φ as shown in (1).

$$S = \Phi X \tag{1}$$

where X is the discrete signal of N elements, Φ is the transformation matrix of $N \times N$ in size, and S is the signal in the sparse domain. There are K non-zero components in S, where $N \gg K$. The CS theory states that M samples can be randomly selected from S, i.e., the matrix Φ is sub-sampled by choosing some random rows/columns. If the sub-matrix chosen from the matrix Φ is $\Lambda_{M \times N}$ where $N \gg M$, then $Y_{M \times 1}$ contains the measurements of the CS [25].

$$Y = \Lambda S = \Lambda \Phi X \tag{2}$$

$$Y = \Theta X \tag{3}$$

where $\Theta_{M \times N} = \Lambda \Phi$ represents the CS matrix. The size of Y is much less the size of X. The choice of Φ must guarantees the property of incoherence, where small number of measurements can provide the reconstruction. In (3) contains more unknowns than equations. An optimization algorithm must be used to reach a solution. Greedy algorithms are commonly used such as convex relaxation [26], orthogonal matching pursuit (OMP) [27], and matching pursuit (MP) [28]. Here, the l_1-minimization is considered, where it expressed as:

$$\min\|X\|_{l_1} \text{ subject to } Y = \Theta X \tag{4}$$

where the l_1 norm of X represents the absolute sum of the components of X

$$\min\|X\|_{l_1} = \sum_{i=1}^{N}|X_i| \tag{5}$$

3.   PSO THEORY

The PSO is widely used in optimization problem, due to its simplicity of implementation [29], [30]. In PSO, several elements in the swarm scan the d-dimensional problem space for new solutions. A vector of position Pi (the particle's indicator), and a velocity vector indicate each particle's position and velocity, respectively. After each iteration, the swarm's best position vector is saved in a vector. In (6) determines the velocity update from the original velocity to the current velocity. In (7) is then used to calculate the current position, which is equal to the sum of the new velocity and the old position [31].

$$v_i(t) = w * v_i(t-1) + C_1 R_1 \left(P_{Best_i}(t) - P_i(t-1) \right) + C_2 R_2 (G_{Best_t} - P_i(t-1)) \qquad (6)$$

$$P_i(t) = P_i(t-1) + v_i(t-1) \qquad (7)$$

Where v_i is the ith particle velocity, w represents the inertia, P_{Best_i} is the best position for the ith particle, G_{Best} is the best position up to the tth iteration, C_1 and C_2 are acceleration factors, and R_1 and R_2 are two random numbers uniformly distributed in the interval between 0 and 1. The size and range of the particles are defined according to the problem. The best fitness must have a lower value than a pre-set threshold [31]. A summary of how a PSO works can be addressed in five steps as follows:

Step 1: Initialize for each particle with velocity and location.
Step 2: Determine the optimal solution; if it is best than P$_{best}$, the current value is equal to P$_{best}$.
Step 3: G$_{best}$ is the best fitness value for particles.
Step 4: Calculate the new velocity and position for each particle according to velocity and position update equations.
Step 5: While the minimum error criteria are not attained, the steps 2 to 4 are repeated until the required target is obtained.

4.   PROPOSED METHOD

The proposed compression method in this paper is a modified version of the method previously presented in [24]. The main difference is that the experimentally tunned thresholds in [24] are PSO optimized in this paper. Figure 1 illustrates the flowchart of the proposed method. The method starts with dividing the image into frames. The DCT is then calculated for each frame, and the sparsity index (SI) is computed for that frame as described in [24]. The next step is compressing each frame using CS, based on its SI value, high SI refers to higher compression level, since the frame contains high sparsity. While low SI refers to low compression level, since is contains low sparsity, i.e., high information.
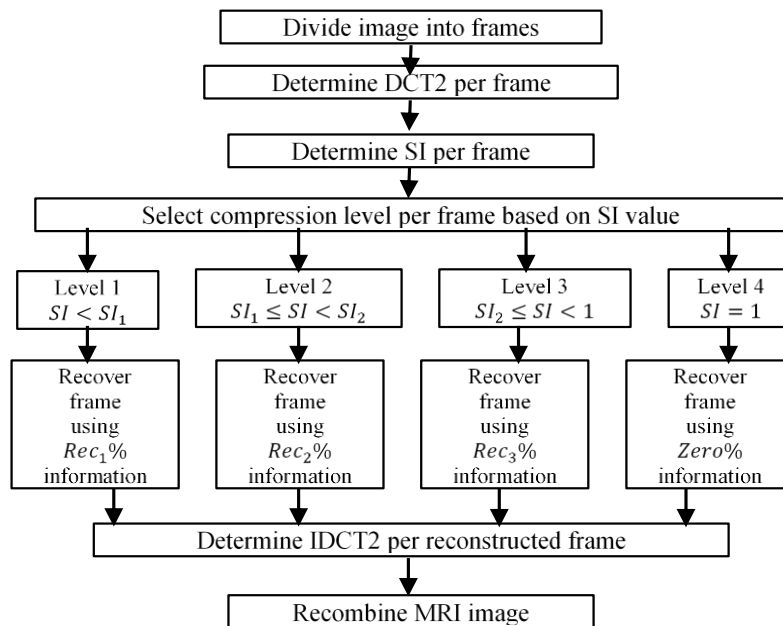

Figure 1. Flowchart of the proposed method

In the reconstruction stage, the CS is considered to recover each frame using a percentage Rec_i of the DCT information, which represents the compressed data of that frame. It can be noticed from Figure 1 that SI_1, SI_2, Rec_1, Rec_2 and Rec_3 are all experimentally chosen in [24]. While in this paper, these parameters are optimized using PSO, to provide a fitness criterion.

5.   FITNESS FUNCTION

The PSO in this paper is designed to maximize a fitness function that considers two main parameters, the peak signal to noise ratio (PSNR) and the compression level (CL). To model such fitness function it is tricky task, since the better solution of the five parameters SI_1, SI_2, Rec_1, Rec_2 and Rec_3 must satisfy a higher PSNR and higher CL. It is well known that in image compression higher PSNR can be only obtained with low CL. While higher CL can be only obtained with low PSNR value. In the proposed method, it is up to the user to decide which parameter to set and which to optimize. For example, the user can set a specific CL value, and the PSO optimizes the five parameters to maximize the PSNR. Alternatively, the user can set a desired PSNR value, and the PSO optimizes the five parameters to maximize the CL. To meet the previous conditions, in this paper a two-dimensional sigmoid function is suggested as follows:

$$F_1 = \frac{500}{1+e^{-t_1(CL-m_1)}+e^{t_1(CL-m_1)}+e^{-t_2(100-PSNR)}+e^{0.75t_2(100-PSNR)}} \tag{8}$$

Where F_1 is the fitness function, that maximizes the PSNR after the user pre-set the CL to a desired value of m_1.

$$F_2 = \frac{500}{1+e^{-t_1(PSNR-m_2)}+e^{t_1(PSNR-m_2)}+e^{-t_2(100-CL)}+e^{0.75t_2(100-CL)}} \tag{9}$$

Where F_2 is the fitness function, that maximizes the CL after the user pre-set the PSNR to a desired value of m_2, t_1 and t_2 are the temperatures factors of the two-dimensional sigmoid function and their values are 10 and 0.04 respectively. Figure 2(a) shows the graph of the suggested fitness function as stated in (8), while Figure 2(b) shows the fitness function as stated in (9).
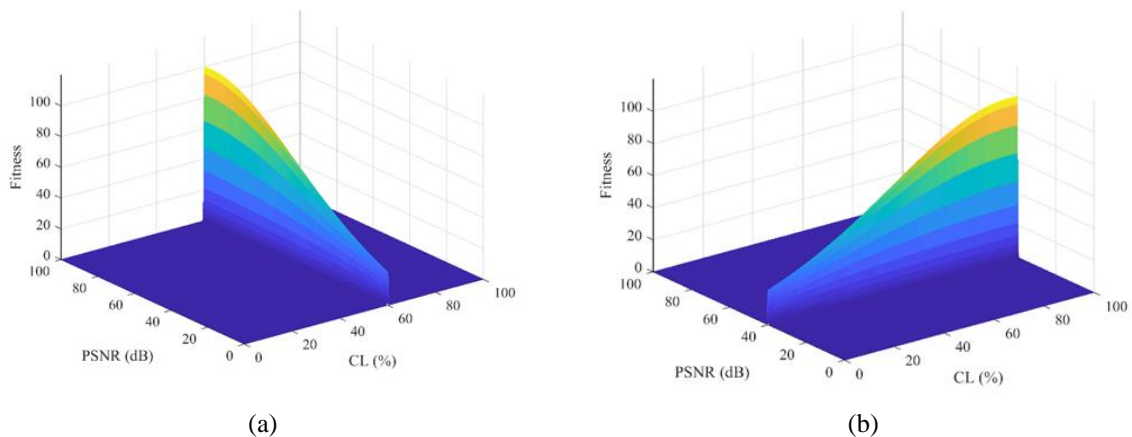

Figure 2. Fitness functions by (a) setting CL to 60% and maximize PSNR and (b) setting PSNR to 40 dB and maximize CL

6.   RESULTS AND DISCUSSION

The same six images, which are previously used in [24] are considered here. These images are named as $Head_{720 \times 720}$, $Neck_{600 \times 600}$, $Brain_{840 \times 840}$, $Ankle_{720 \times 720}$, $Hand_{460 \times 720}$, and $Knee_{720 \times 720}$ as shown in Figures 3(a)-(f). A segmentation of 10×10 pixels is applied on each image, then the CS compression is performed as explained in Figure 1. Each MRI image has a trade-off curve between the CL and the PSNR. Here, F_2 as expressed in (9), is considered as the fitness function for the PSO. The PSO parameters are listed in Table 1.

Table 1. PSO parameters

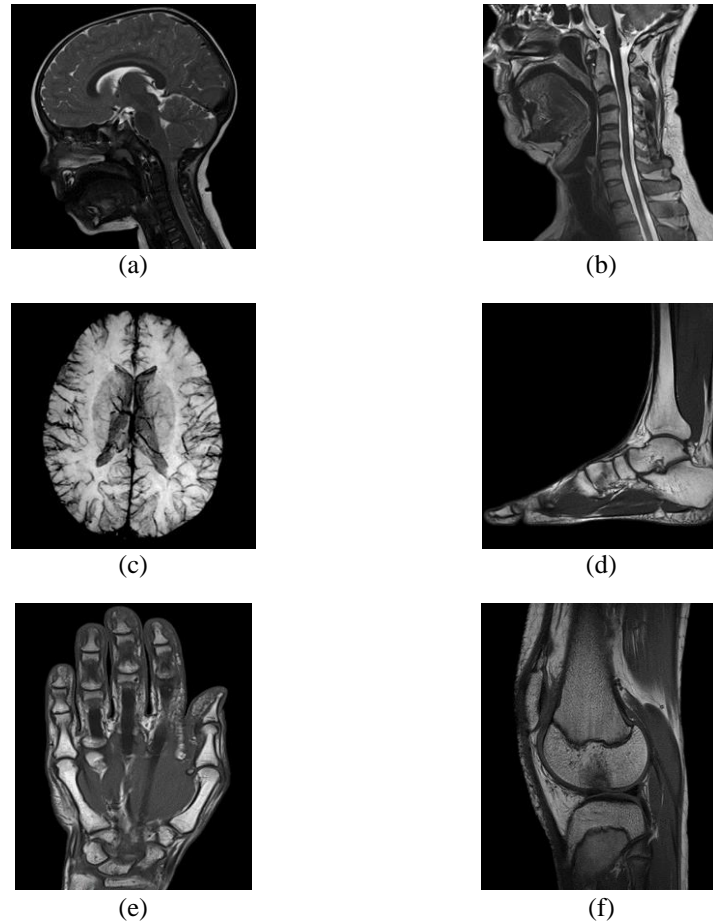| Parameter	Value
C_1	1.5
C_2	2.5
w	0.6
Swarm size	10
Iterations	10

Figure 3. MRI images, (a) head, (b) neck, (c) brain, (d) ankle, (e) hand, and (f) knee

Figures 4(a)-(f) (see in Appendix) shows the trade-off curve for each image, in the case of using uniform compression (i.e., compressing the whole image with one CL), and in the case of using the proposed method, where multilevel CS compression is used, and the tuneable parameters SI_1, SI_2, Rec_1, Rec_2 and Rec_3 are optimized using the PSO for each image, at a desired PSNR.

It can be noticed from Figure 4(a)-(f) (see in Appendix) that the proposed method has superior performance at high PSNR values, when compared to uniform compression. However, the difference in CL decreases between the two at low PSNR values. Practically, the user of the compression proposed method can decide the desired PSNR value, while the method optimizes for highest possible CL value.

7. CONCLUSIONS

This paper presents a modification on the compression method, previously presented in [24]. The proposed method employs PSO, to optimize the amount of information for the CS reconstruction, at each level of compression Rec_1, Rec_2 and Rec_3. In addition, the PSO optimizes the thresholds of the sparsity, that separate the levels of compression SI_1 and SI_2. A two-dimensional sigmoid function is suggested, as fitness function for the PSO. The main advantage of the proposed method, is the flexibility in setting different PSNR value, to achieve the highest possible CL.

ACKNOWLEDGEMENTS

APPENDIX
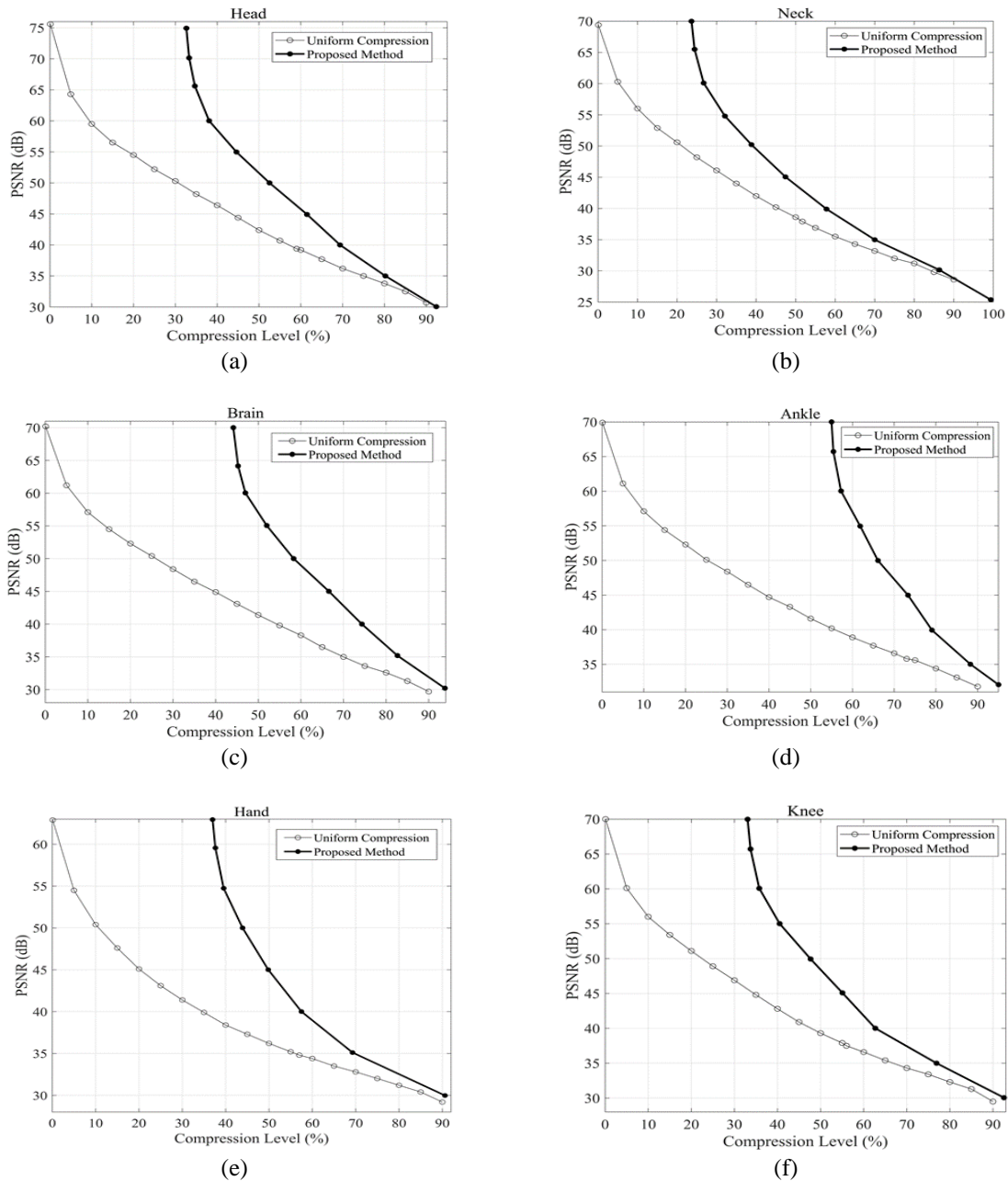
Figure 4. Proposed method performance versus uniform compression (a) head, (b) neck, (c) brain, (d) ankle, (e) hand, and (f) knee

REFERENCES

[1]   E. J. Candès, "Compressive sampling," in *Proceedings of the international congress of mathematicians*, vol. 3, pp. 1433-1452, 2006, doi: 10.4171/022-3/69.
[2]   D. L. Donoho, "Compressed sensing," in *IEEE Transactions on Information Theory*, vol. 52, no. 4, pp. 1289-1306, April 2006, doi: 10.1109/TIT.2006.871582.

[3]   E. Hot and P. Sekulić, "Compressed sensing MRI using masked DCT and DFT measurements," *2015 4th Mediterranean Conference on Embedded Computing (MECO)*, 2015, pp. 323-326, doi: 10.1109/MECO.2015.7181934.

[4]   M. Alzahrani and M. Albinali, "Comparative Analysis of Lossless Image Compression Algorithms based on Different Types of Medical Images," *2021 International Conference of Women in Data Science at Taif University (WiDSTaif)*, 2021, pp. 1-6, doi: 10.1109/WiDSTaif52235.2021.9430242.

[5]   S. Guruprasad, S. Bharathi, and D. A. R. Delvi, "Effective compressed sensing MRI reconstruction via hybrid GSGWO algorithm," *Journal of Visual Communication and Image Representation,* vol. 80, p. 103274, 2021, doi: 10.1016/j.jvcir.2021.103274.

[6]   M. Golbabaee *et al.*, "Compressive MRI quantification using convex spatiotemporal priors and deep encoder-decoder networks," *Medical Image Analysis,* vol. 69, p. 101945, 2021, doi: 10.1016/j.media.2020.101945.

[7]   M. Ragab, O. A. Omer, and M. Abdel-Nasser, "Compressive sensing MRI reconstruction using empirical wavelet transform and grey wolf optimizer," *Neural Computing and Applications,* vol. 32, no. 7, pp. 2705-2724, 2020, doi: 10.1007/s00521-018-3812-7.

[8]   D.-O. Kim and R.-H. Park, "Evaluation of image quality using dual-tree complex wavelet transform and compressive sensing," *Electronics letters,* vol. 46, no. 7, pp. 494-495, 2010, doi: 10.1049/el.2010.3452.

[9]   J. Xu, Y. Qiao, Q. Wen, and Z. Fu, "Perceptual rate-distortion optimized image compression based on block compressive sensing," *Journal of Electronic Imaging,* vol. 25, no. 5, p. 053004, 2016, doi: 10.1117/1.JEI.25.5.053004.

[10]   D. Rontani, D. Choi, C.-Y. Chang, A. Locquet, and D. Citrin, "Compressive sensing with optical chaos," *Scientific reports,* vol. 6, no. 1, pp. 1-7, 2016, doi: 10.1038/srep35206.

[11]   V. Unni, D. Mishra, and G. Subrahmanyam, "Adaptive multifocus image fusion using block compressed sensing with smoothed projected Landweber integration in the wavelet domain," *Journal of the Optical Society of America A,* vol. 33, no. 12, pp. 2516-2525, 2016, doi: 10.1364/JOSAA.33.002516.

[12]   N. Eslahi, A. Aghagolzadeh, and S. M. H. Andargoli, "Image/video compressive sensing recovery using joint adaptive sparsity measure," *Neurocomputing,* vol. 200, pp. 88-109, 2016, doi: 10.1016/j.neucom.2016.03.013.

[13]   N. Zhou, S. Pan, S. Cheng, and Z. Zhou, "Image compression–encryption scheme based on hyper-chaotic system and 2D compressive sensing," *Optics & Laser Technology,* vol. 82, pp. 121-133, 2016, doi: 10.1016/j.optlastec.2016.02.018.

[14]   M. A. Qureshi and M. Deriche, "A new wavelet based efficient image compression algorithm using compressive sensing," *Multimedia Tools and Applications,* vol. 75, no. 12, pp. 6737-6754, 2016, doi: 10.1007/s11042-015-2590-9.

[15]   R. Liang, L. Kang, J. Huang, and J. Huang, "Reconstruction for infrared image based on block-sparse compressive sensing," in *2016 IEEE 13th International Conference on Signal Processing (ICSP)*, 2016, IEEE, pp. 719-722, doi: 10.1109/ICSP.2016.7877926.

[16]   M. V. R. Manimala, C. D. Naidu and M. N. Giriprasad, "Sparse recovery algorithms based on dictionary learning for MR image reconstruction," *2016 International Conference on Wireless Communications, Signal Processing and Networking (WiSPNET)*, 2016, pp. 1354-1360, doi: 10.1109/WiSPNET.2016.7566358.

[17]   C. H. Chang, X. Yu, and J. X. Ji, "Compressed sensing MRI reconstruction from 3D multichannel data using GPUs," *Magnetic resonance in medicine,* vol. 78, no. 6, pp. 2265-2274, 2017, doi: 10.1002/mrm.26636.

[18]   M. Lustig, D. L. Donoho, J. M. Santos and J. M. Pauly, "Compressed Sensing MRI," in *IEEE Signal Processing Magazine*, vol. 25, no. 2, pp. 72-82, March 2008, doi: 10.1109/MSP.2007.914728.

[19]   S. D. Babacan, X. Peng, X. -P. Wang, M. N. Do and Z. -P. Liang, "Reference-guided sparsifying transform design for compressive sensing MRI," *2011 Annual International Conference of the IEEE Engineering in Medicine and Biology Society*, 2011, pp. 5718-5721, doi: 10.1109/IEMBS.2011.6091384.

[20]   S. F. Roohi, D. Zonoobi, A. A. Kassim and J. L. Jaremko, "Dynamic MRI reconstruction using low rank plus sparse tensor decomposition," *2016 IEEE International Conference on Image Processing (ICIP)*, 2016, pp. 1769-1773, doi: 10.1109/ICIP.2016.7532662.

[21]   F. A. Razzaq, S. Mohamed, A. Bhatti, and S. Nahavandi, "Non-uniform sparsity in rapid compressive sensing MRI," in *2012 IEEE International Conference on Systems, Man, and Cybernetics (SMC)*, 2012, pp. 2253-2258, doi: 10.1109/ICSMC.2012.6378076.

[22]   F. A. Razzaq, S. Mohamed, A. Bhatti and S. Nahavandi, "Locally Sparsified Compressive Sensing for Improved MR Image Quality," *2013 IEEE International Conference on Systems, Man, and Cybernetics*, 2013, pp. 2163-2167, doi: 10.1109/SMC.2013.370.

[23]   S. H. Safavi and F. Torkamani-Azar, "Sparsity-aware adaptive block-based compressive sensing," *IET Signal Processing,* vol. 11, no. 1, pp. 36-42, 2017, doi: 10.1049/iet-spr.2016.0176.

[24]   T. Tashan and M. A.-Azawi, "Multilevel magnetic resonance imaging compression using compressive sensing," *IET Image Processing,* vol. 12, no. 12, pp. 2186-2191, 2018, doi: 10.1049/iet-ipr.2018.5611.

[25]   R. Chartrand, "Fast algorithms for nonconvex compressive sensing: MRI reconstruction from very few data," *2009 IEEE International Symposium on Biomedical Imaging: From Nano to Macro*, 2009, pp. 262-265, doi: 10.1109/ISBI.2009.5193034.

[26]   S. S. Chen, D. L. Donoho, and M. A. Saunders, "Atomic decomposition by basis pursuit," *Society for Industrial and Applied Mathematics review,* vol. 43, no. 1, pp. 129-159, 2001, doi: 10.1137/S003614450037906X.

[27]   S. G. Mallat and Zhifeng Zhang, "Matching pursuits with time-frequency dictionaries," in *IEEE Transactions on Signal Processing*, vol. 41, no. 12, pp. 3397-3415, Dec. 1993, doi: 10.1109/78.258082.

[28]   J. A. Tropp and A. C. Gilbert, "Signal recovery from random measurements via orthogonal matching pursuit," *IEEE Transactions on information theory,* vol. 53, no. 12, pp. 4655-4666, 2007, doi: 10.1109/TIT.2007.909108.

[29]   J. Kennedy and R. Eberhart, "Particle swarm optimization," *Proceedings of ICNN'95 - International Conference on Neural Networks*, 1995, pp. 1942-1948 vol.4, doi: 10.1109/ICNN.1995.488968.

[30]   S. Kadry, V. Rajinikanth, J. Koo, and B.-G. Kang, "Image multi-level-thresholding with Mayfly optimization," *International Journal of Electrical & Computer Engineering (2088-8708),* vol. 11, no. 6, 2021, doi: 10.11591/ijece.v11i6.pp5420-5429.

[31]   S. Sumathi and S. Paneerselvam, "Computational intelligence paradigms: theory & applications using MATLAB," CRC Press, 2019.

BIOGRAPHIES OF AUTHORS

Tariq Tashan 🆔 [g] [SC] [P] is a lecturer at the Electrical Engineering department, Mustansiriyah University, Baghdad-Iraq. He obtained his BSc in Electrical Engineering and MSc in Communication and Electronics from Mustansiriyah University. He obtained his PhD in Biologically Inspired Speaker Verification from Nottingham Trent University, Nottingham, United Kingdom, and he is Member of the Institution of Engineering and Technology (MIET). His research interests include speaker recognition, image processing, pattern recognition, optimization, and neural networks. He can be contacted at email: tariq.tashan@uomustansiriyah.edu.iq.

Ahmed K. Kadhim 🆔 [g] [SC] [P] was born in Baghdad, Iraq, in 1987. He received the B.E. degree in electrical engineering from the University of Mustansiriyah, Baghdad, Iraq, in 2009, and the M.Sc. degrees in microelectronic engineering from the Newcastle University, UK, in 2016. In 2012, he joined the Department of Electrical Engineering, University of Mustansiriyah, as a demonstrator in the electronic laboratory, and in 2016 became a Lecturer. His current research interests include μsystems, embedded systems, and processors, internet of things (IoT), cloud computing, sensors, robotics design. He can be contacted at email: a.k.kadhim@uomustansiriyah.edu.iq.